A Molecular Tool for Measuring the Electron-Acceptor Ability of Ligands from Crystallographic Data

Francesco P. Fanizzi,*[a] Nicola Margiotta,[b] Maurizio Lanfranchi,[c] Antonio Tiripicchio,[c] Gianfranco Pacchioni,[d] and Giovanni Natile*[b]

Keywords: Ab initio calculations / NMR spectroscopy / Pi ligands / Platinum / X-ray diffraction

A method is proposed for the direct measurement of the π-acidity of ligands coordinated to a metal center. The four-coordinate complex $[PtI_2(Me_2\text{-phen})]$ (Me_2-phen = 2,9-dimethyl-1,10-phenanthroline) is unique since it behaves as a molecular trap and, in the presence of a nucleophile (L), one end of it dissociates to allow the L ligand to coordinate *trans* to the monocoordinated diamine. The coordination of the free end of the phenanthroline is impeded by the filled d orbitals of the metal lying in the same plane as the phenanthroline (d_{yz} and d_{z^2} electrons assuming as x-axis that of the I–Pt–I vector). However, if the L ligand is a π-acid able to remove electron charge from the yz plane, the second end of the phenanthroline will also be able to interact with platinum. A linear correlation is found between the crystallographic N–Pt–L angle (180° in ideal square-planar species and 143° in a trigonal bipyramid with a bite angle for bidentate Me_2-phen of 74°) and the π-acceptor capacity of the L ligand as estimated by ab initio calculations. Alkenes and alkynes are found to be among the best π-acids and lead to a regular trigonal-bipyramidal five-coordinate species. CO appears to be only halfway in between the best π-acceptor ligands and those with smallest π-acidity. P-, S-, and N-donor ligands follow in that order without significant differences between sulfides and sulfoxides or between aliphatic amines and pyridine. The very small difference between aliphatic amines and pyridine has been confirmed by investigation of the rate of exchange between the two ends for monocoordinated phenanthroline by ^1H NMR spectroscopy. The activation energy ($\Delta G^{\ddagger}$) was found to be equal, within the experimental error, for the two types of *trans* ligands.
(© Wiley-VCH Verlag GmbH & Co. KGaA, 69451 Weinheim, Germany, 2004)

1. Introduction

The π-acceptor ability of a ligand is a key factor in determining its *trans* effect in substitution reactions involving square-planar complexes.[1] A π-acceptor ligand, one that is able to draw electron charge from the metallic center, stabilizes the trigonal-bipyramidal transition state in which the π-acceptor ligand, its *trans* ligand, and the incoming nucleophile share the trigonal plane. The accepted order of *trans*-labilizing ligands is: C_2H_4, CO > CN^- > NO_2^- > SCN^- > I^- > Br^- > Cl^- > NH_3 > OH^-.[2] This series has been derived mainly from kinetic experiments, however it would be highly desirable to have a direct means of measuring the ability of a ligand to favor the assembly of three ligands in the trigonal plane of a five-coordinate geometry.

In investigating the reaction of the sterically strained and highly reactive complexes $[PtX_2(Me_2\text{-phen})]$ (X = Cl, Br, I; Me_2-phen = 2,9-dimethyl-1,10-phenanthroline)[3,4] with an incoming nucleophile, it was found that, contrary to all expectations, no substitution takes place but, instead, simple addition of the extra ligand occurs, with formation of $[PtX_2(Me_2\text{-phen})(L)]$ species.[5–8] Depending upon the characteristics of the incoming ligand, the phenanthroline may become monodentate (and the platinum center still be four-coordinate) or can remain bidentate (and the platinum center become five-coordinate). Preliminary X-ray structural results concerning *trans*-$[PtX_2(Me_2\text{-phen})(L)]$ complexes (X = Cl, L = C_2H_4; X = I, L = CO, PPh_3, and PhNO) showed that the geometry of the complex can range from trigonal bipyramidal (L = ethylene) to square planar (L = PhNO).[5]

We have hypothesized that the structural data of this series of complexes can offer a direct way to rank the π-acceptor ability of L ligands and have extended the investigation to several L ligands comprising the most common S- (sulfides, sulfoxides) and N-donor ligands (aliphatic am-

---

[a] Dipartimento di Scienze e Tecnologie Biologiche ed Ambientali, Università di Lecce,
Via Monteroni 73100, Lecce, Italy
E-mail: fp.fanizzi@unile.it
[b] Dipartimento Farmaco-Chimico, Università degli Studi di Bari,
Via E. Orabona 4, 70125 Bari, Italy
E-mail: natile@farmchim.uniba.it
[c] Dipartimento di Chimica Generale ed Inorganica, Chimica Analitica, Chimica Fisica, Università di Parma,
Parco Area delle Scienze 17/A, 43100 Parma, Italy
[d] Dipartimento di Scienza dei Materiali, Università di Milano-Bicocca,
Via R. Cozzi 53, 20125 Milano, Italy

DOI: 10.1002/ejic.200300888

ines and pyridine). In this paper we combine accurate X-ray diffraction data of a wide series of *trans*-[PtI_2(Me_2-phen)(L)] complexes with the results of ab initio calculations to show that there is a linear relationship between the stereochemistry of the phenanthroline and the π-acidity of the *trans* ligand. The calculations are aimed at providing a quantum-mechanical rationale for the observed trends more than to give quantitative estimates of the observable properties.

The paper is organized as follows. In Section 2a we describe the synthesis and NMR studies of the complexes under investigation. Section 2b is dedicated to the structure of the complexes from X-ray diffraction measurements. Section 2c is devoted to the calculations and to the quantitative estimate of the π-acceptor ability of the L ligands. The existence of a direct correlation between the N−Pt−L angle and the π-acceptor ability is shown and discussed in the concluding Section 3.

2. Results

2a. Synthetic Aspects and NMR Measurements

[PtI_2(Me_2-phen)] (**1**) reacts instantaneously with an extra ligand (L) to give the corresponding addition product [PtI_2(Me_2-phen)(L)] (**2**). The addition reaction is quantitative for L = C_2H_4 (**a**), $C_2(C_6H_5)_2$ (**b**), CO (**c**), $P(C_6H_5)_3$ (**d**), $H_2(C_3H_7)N$ (**g**), and C_5H_5N (**h**). In the case of L = $(CH_3)_2SO$ (**e**) and $(CH_3)_2S$ (**f**) an excess of L ligand is required in order to obtain complete conversion into the addition product. The direct displacement of one end of the Me_2-phen ligand by the incoming ligand (L) by the usual S_N2 mechanism would place L *cis* to the monodentate Me_2-phen (upper row of Scheme 1). In some instances (L = PPh_3), such a species has been detected in solution, but not as the major reaction product. Moreover it is not an intermediate leading to the species with PPh_3 *trans* to monocoordinated Me_2-phen but it reacts further placing a second molecule of PPh_3 *trans* to the first one.[6] However, the L ligand is most commonly found *trans* to the monodentate Me_2-phen, an indication that one end of Me_2-phen is first released and the transient T-shaped three-coordinate species isomerizes from *cis* to *trans* conformation before addition of L (lower row of Scheme 1). Most of the data thus far accumulated indicate that such a dissociative mechanism can be operative even in four-coordinate square-planar complexes.[9−13]

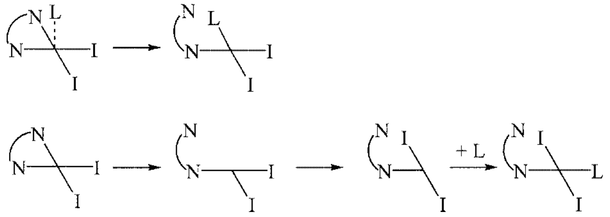

Scheme 1

It has been found that, depending upon the nature of the L ligand, the phenanthroline can assume the whole range of positions spanning from pure monodentate to perfectly symmetrical bidentate coordination. This aspect will be treated in detail in Section 2b devoted to the crystal structure analysis. NMR spectroscopy is not very informative in this respect since, even in the case of monocoordinated Me_2-phen, a fast rate of exchange between the free and coordinated ends can render the two halves of the phenanthroline equivalent on the NMR timescale, as in the case of five-coordinate species. However in the case of pyridine and *n*-propylamine complexes, the single set of proton resonances observed for Me_2-phen at room temperature is split into two sets (one for each inequivalent half of Me_2-phen) by lowering the temperature to 210 K (Table 1). In these two cases dynamic NMR spectroscopy[14,15] allowed to calculate the rate constants (*k*) for the exchange between the free and coordinated ends of the phenanthroline and, from the dependence of the rate constants upon the temperature, it was possible to evaluate the activation parameters ($\Delta H^{\ddagger}$, $\Delta S^{\ddagger}$, and therefrom $\Delta G^{\ddagger}$ at a given temperature T, $\Delta G^{\ddagger}_{T}$). $\Delta G^{\ddagger}_{T}$ corresponds to the free-energy difference between the ground state (the four-coordinate species) and the transition state (the latter is likely to be close to a transition species with both ends of the phenanthroline symmetrically bound to platinum).

The NMR spectra of [PtI_2(Me_2-phen)(py)] (**2g**) recorded at different temperatures (black lines) overlapped by the simulated spectra (grey lines) are reported in Figure 1. Plots of $\ln(k/T)$ versus $1/T$ are reported in Figure 2. Values of $\Delta H^{\ddagger} = 57 \pm 2\ \mathrm{kJ{\cdot}mol^{-1}}$, $\Delta S^{\ddagger} = 20 \pm 2\ \mathrm{J{\cdot}mol^{-1}{\cdot}K^{-1}}$, and $\Delta G^{\ddagger}_{295} = 51 \pm 2\ \mathrm{kJ{\cdot}mol^{-1}}$ were found for the pyridine complex **2g**, while values of $\Delta H^{\ddagger} = 56 \pm 2\ \mathrm{kJ{\cdot}mol^{-1}}$, $\Delta S^{\ddagger} = 14 \pm 2\ \mathrm{J{\cdot}mol^{-1}{\cdot}K^{-1}}$, and $\Delta G^{\ddagger}_{295} = 52 \pm 2\ \mathrm{kJ{\cdot}mol^{-1}}$ were found for the *n*-propylamine complex **2h**. The very small difference between the $\Delta G^{\ddagger}_{295}$ values for compounds **2g** and **2h** indicates that the ability to stabilize the trigonal bipyramidal transition state, and hence their π-acceptor capacity towards electrons confined in the trigonal plane, can be considered equivalent for the two ligands and, in general, for aliphatic amines and pyridine.

2b. Crystal Structures of Complexes 2a, 2e, 2f, 2g, and 2h

The molecular structures of **2a** (L = C_2H_4), **2e** (L = DMSO), **2f** (L = DMS), **2g** (L = Py), and **2h** (L = NH_2nPr) are depicted in Figure 3, 4, 5, 6, and 7, respectively. Selected bond lengths and angles are summarized in Table 2 for all compounds.

In **2a** the Pt atom presents a trigonal bipyramidal coordination geometry in which the two N atoms of the bidentate Me_2-phen ligand and the double bond of the ethylene molecule are the equatorial donors and the two iodine atoms the axial ligands (Figure 3). The complex has pseudo-C_{2v} symmetry with the pseudo-twofold axis passing through the midpoint of the ethylene ligand and the Pt atom. The bond lengths and angles in the coordination sphere are normal

Table 1. ^{1}H NMR chemical shifts (ppm) for free Me$_2$-phen, [PtI$_2$(Me$_2$-phen)] (**1**), and [PtI$_2$(Me$_2$-phen)(L)] (**2**) complexes in CDCl$_3$ [a]

Compound	Temp. (K)	H(4/7)	H(5/6)	H(3/8)	CH$_3$(2/9)	L
Me$_2$-phen	298	8.11 d (8)	7.70 s	7.47 d (8)	2.93 s	–
[PtI$_2$(Me$_2$-phen)] (**1**)	298	8.33 d (8)	7.79 s	7.57 d (8)	3.25 s [7]	–
L = C$_2$H$_4$ (**2a**)	298	8.25 d (8)	7.85 s	7.79 d (8) [3]	3.44 s [7]	4.20 [71]
L = (CH$_3$)$_2$SO (**2e**)	293	8.20 d (8)	7.76 s	7.46 d (8)	3.46 s [7]	4.04 [22]
L = (CH$_3$)$_2$S (**2f**)	298	8.13 d (8)	7.75 s	7.60 d (8)	3.42 s [7]	2.83 s [42]
L = C$_5$H$_5$N (**2g**)	295	8.19 d (8)	7.78 s	7.63 d (8)	3.58 br	9.45 d (8) [33] (*o*), 7.75 t (*p*), 7.23 (*m*)
	213	H(4), 8.32 d (8) H(7), 8.20 d (8)	H(5), 7.89 s H(6), 7.88 s	H(3), 7.70 d (8) H(8), 7.62 d (8)	Me(2), 3.81 s Me(9), 2.83 s	9.28 d (8) (*o*), 7.78 t (8) (*p*), 7.35 d (8) (*m*)
L = H$_2$(C$_3$H$_7$)N (**2h**)	293	8.09 d (8)	7.71 s	7.55 d (8)	3.45 br	1.00 t (8), 1.62 m (8), 3.16 m, 3.62 br
	203	H(4), 8.19 d (8) H(7), 8.12 d (8)	H(5), 7.83 d H(6), 7.70 d	H(3), 7.64 d (8) H(8), 7.59 d (8)	Me(2), 3.70 s [38] Me(9), 2.98 s	0.87 t (8), 1.55 m, 3.10 m, 3.05 m

[a] $J_{Pt,H}$ (Hz) in square brackets and $^3J_{H,H}$ (Hz) in parentheses when assignable, s = singlet, d = doublet, t = triplet, m = multiplet, br = broad, (*o*) = *ortho*, (*m*) = *meta*, and (*p*) = *para.*

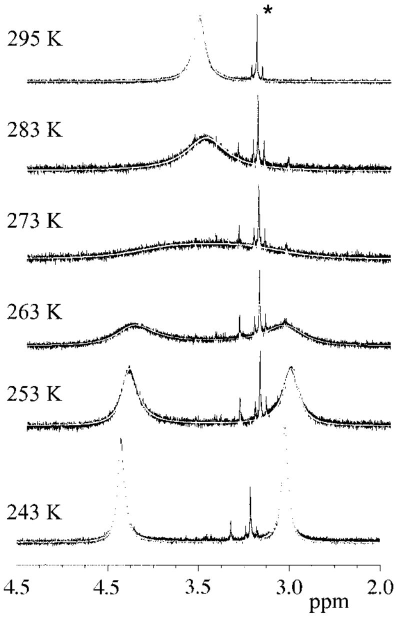

Figure 1. Experimental (black line) and simulated (grey line) ^{1}H NMR spectra (only the aliphatic region is shown) of [PtI$_2$(Me$_2$-phen)(py)] (**2g**) in CDCl$_3$ at different temperatures; the asterisk indicates the peak belonging to a small excess of the starting complex [PtI$_2$(Me$_2$-phen)] (**1**)

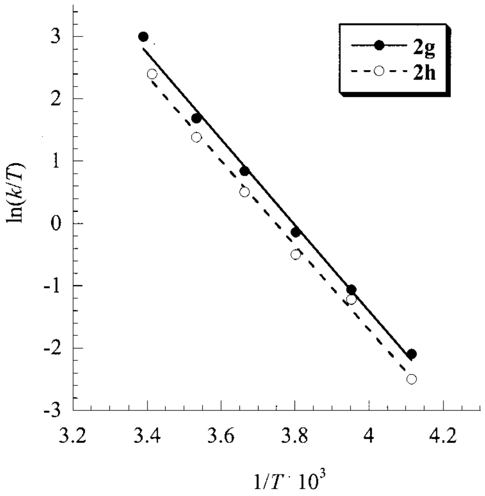

Figure 2. Plots of ln(*k*/T) as a function of 1/T for compounds **2g** and **2h** (*k* values obtained from the line shape analysis of the simulated NMR spectra)

and very similar to those found in the related dichloro derivative.[5]

In **2e** the L ligand is an S-coordinated DMSO molecule (Figure 4) while in **2f** it is dimethyl sulfide (Figure 5). In both complexes the Pt atom shows a slightly distorted square-planar coordination with the L ligand *trans* to the N1-coordinated phenanthroline; two *trans* iodo ligands complete the coordination sphere. In **2e** the orientation of the DMSO molecule is such that a methyl group is placed in the coordination plane [C(15)−S−Pt−I(1) torsion angle of 3.1(4)°] and is responsible for the increase in the S−Pt−I(1) angle with respect to the S−Pt−I(2) angle [96.47(8)° and 89.15(8)°, respectively]. The two Pt−I bond lengths are also significantly different [Pt−I(1) = 2.617(1) and Pt−I(2) = 2.650(1) Å]. A similar situation is found in **2f** [C(15)−S−Pt−I(1) torsion angle of 23.6(4)°, S−Pt−I(1) angle of 96.27(7)°, and S−Pt−I(2) angle of 85.90(7)°]. The phenanthroline is not perfectly planar but shows a certain degree of twist [displacements of the methyl carbon atoms C(13) and C(14) from the mean plane of the phenanthroline of 0.22(1) and −0.22(1) Å for **2e** and 0.25(1) and −0.18(1) Å for **2f**]. This type of phenanthroline deformation is also present in **2a**, but to a smaller extent [deviations from the mean plane of −0.16(1) and 0.14(1) Å for C(13) and C(14), respectively]. In both compounds **2e** and **2f** the Pt atom is slightly out of the mean coordination plane and displaced towards the N(2) atom of the phenanthroline [Pt···N(2) distance of 2.629(6) and 2.666(6) Å for **2e** and **2f**, respectively]. Thus the coordination can be defined as elongated square pyramidal (4+1). The degree of transition from four coordination to five coordination can be judged from the N(1)−Pt−S angle [170.58(17)° and 169.89(17)° for **2e** and

Table 2. Selected bond lengths (Å) and angles (°) for **2a**, **2e**, **2f**, **2g**, and **2h**

Compound	[PtI_2(Me_2-phen)(C_2H_4)] (**2a**)	[PtI_2(Me_2-phen)(DMSO) (**2e**)	[PtI_2(Me_2-phen)(DMS)] (**2f**)	[PtI_2(Me_2-phen)(py)] (**2g**)	[PtI_2(Me_2-phen)(NH_2*n*Pr)] (**2h**)
Pt−I(1)	2.6169(13)	2.6171(14)	2.6239(14)	2.6286(13)	2.6310(12)
Pt−I(2)	2.6240(13)	2.6495(13)	2.6395(13)	2.6091(13)	2.6073(13)
Pt−L	1.957(3)[a]	2.200(2)	2.264(2)	2.026(5)	2.030(8)
Pt−N(1)	2.236(6)	2.108(6)	2.093(5)	2.037(4)	2.043(8)
Pt−N(2)	2.238(6)	2.629(6)	2.666(6)	2.684(5)	2.641(7)
I(1)−Pt−I(2)	179.32(3)	173.13(2)	175.39(2)	170.97(2)	171.03(3)
N(1)−Pt−I(1)	89.60(18)	86.05(18)	88.44(17)	92.07(13)	92.2(2)
N(1)−Pt−I(2)	90.05(18)	87.78(18)	88.79(17)	86.90(13)	90.4(2)
N(2)−Pt−I(1)	90.11(16)	92.21(14)	91.01(13)	88.58(12)	92.06(17)
N(2)−Pt−I(2)	90.35(16)	88.67(14)	91.57(13)	99.60(11)	96.90(17)
N(1)−Pt−L	143.1(4)[a]	170.58(17)	169.89(17)	176.52(17)	178.6(3)
N(1)−Pt−N(2)	74.1(2)	71.3(2)	71.1(2)	71.9(2)	72.4(3)
I(1)−Pt−L	90.3(4)[a]	96.47(8)	96.27(7)	91.40(14)	89.0(3)
I(2)−Pt−L	89.6(4)[a]	89.15(8)	85.90(7)	89.71(14)	88.3(3)

[a] With respect to the midpoint of the C=C bond.

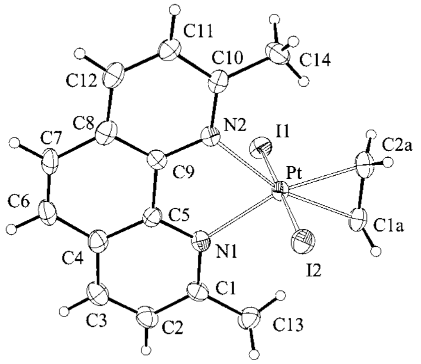

Figure 3. ORTEP view of the molecular structure of [PtI_2(Me_2-phen)(C_2H_4)] (**2a**), thermal ellipsoids are drawn at 30% probability level

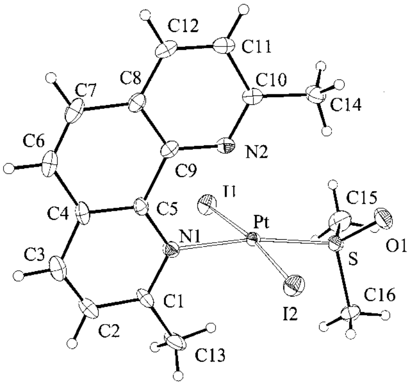

Figure 4. ORTEP view of the molecular structure of [PtI_2(Me_2-phen)(DMSO)] (**2e**), thermal ellipsoids are drawn at 30% probability level

2f, respectively]. The expected values are 180° for a regular square-planar species and 143° for a trigonal bipyramidal species in which the bite angle of the bidentate Me_2-phen lying in the trigonal plane is 74°. The Pt−N(1) bond lengths are similar within experimental errors [2.108(6) and 2.094(5) Å for **2e** and **2f**, respectively] and are in agreement with a comparable *trans* influence of the two ligands. In contrast, the Pt−S distances are significantly different [2.200(2) and 2.264(2) Å for **2e** and **2f**, respectively] reflecting the different oxidation state of the sulfur atom in DMSO and DMS.

The molecular structures of **2g** (L = py) and **2h** (L = NH_2*n*Pr) are depicted in Figure 6 and 7, respectively. The square-planar coordination of the Pt atoms is less distorted than that observed in the previous two cases. The steric bulk of the pyridine and propylamine ligands with respect to the *cis* iodo ligand, is small, and therefore both I−Pt−L angles are close to 90°; this was not the case for the DMSO and DMS complexes previously considered. In **2g** there is an apparent interaction between the pyridine and the phenanthroline ligands so that the planes of the two ligands are canted on the coordination plane in opposite directions and make a dihedral angle of 30.1(2)°. This steric interaction results in a greater twisting of the phenanthroline in **2g** than in **2e** and **2f** [displacement of the C(14) and C(13) carbon atoms from the mean plane of the phenanthroline of

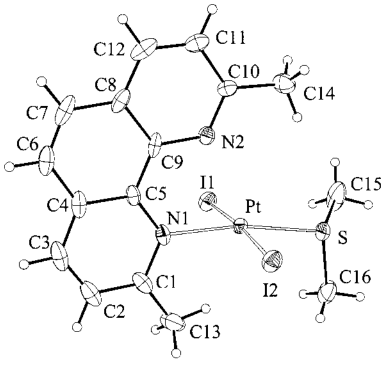

Figure 5. ORTEP view of the molecular structure of [PtI_2(Me_2-phen)(DMS)] (**2f**), thermal ellipsoids are drawn at 30% probability level

−0.35(1) Å and 0.19(1) Å, respectively]. In **2h** the propyl group of the $H_2(C_3H_7)N$ ligand extends into the half space of the coordination plane opposite to that of the N(2) atom and is *quasi* orthogonal to the coordination plane [I(1)−Pt−N(3)−C(15) torsion angle of −88.0(8)°]. The phenanthroline is perfectly planar and makes a dihedral angle of 88.4(1)° with the coordination plane. The degree of transition from four- to five-coordination is smaller in **2g** and **2h** than it was in **2e** and **2f**; moreover there is a small difference between **2g** and **2h** [N(1)−Pt−N(3) angles of 176.5(2)° and 178.6(3)° for **2g** and **2h**, respectively]. Despite the different hybridization of the L donor atom (sp^2 and sp^3 for **2g** and **2h**, respectively) the Pt−N(3) bond length is similar for the two compounds (Table 2). Also the *trans* influence appears to be rather similar for the two compounds as indicated by the values of the Pt−N(1) bond lengths, which are equal within experimental errors. Moreover the Pt−N(1) bond lengths are about 0.06 Å shorter in **2g** and **2h** than they were in **2e** and **2f**, consistent with a greater *trans* influence of S-donor ligands with respect to N-donor ligands.

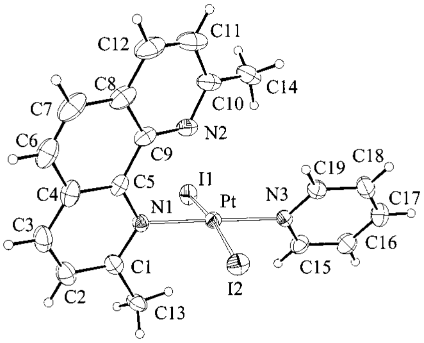

Figure 6. ORTEP view of the molecular structure of $[PtI_2(Me_2\text{-}phen)(py)]$ (**2g**), thermal ellipsoids are drawn at 30% probability level

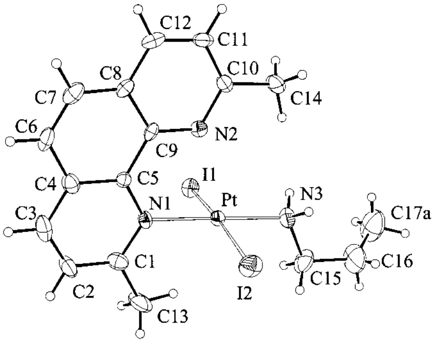

Figure 7. ORTEP view of the molecular structure of $[PtI_2(Me_2\text{-}phen)(NH_2Pr^n)]$ (**2h**), thermal ellipsoids are drawn at 30% probability level

2c. Ab initio Calculations

Ab initio calculations were carried out with the aim of confirming that the observed solid-state molecular structures correspond to the computed ground-state structures and correlating the switch from a four-coordinate (monodentate Me_2-phen) to a five-coordinate structure (bidentate Me_2-phen) with the electronic properties of the L ligand. The calculations were performed at the Hartree−Fock level in order to take advantage of an energy partitioning described below and implemented at this level of theory in a computer code available to us. The use of the HF approach implies the neglect of correlation effects. While this certainly affects some of the computed properties, the physics of the interaction is properly described.

A direct comparison between the results of the geometry optimization and those of the X-ray structures is given in Table 3. In general, the agreement between the ab initio HF and the experimental results is good, in particular as far as the Pt−N(2) distance and the N(1)−Pt−L angle — the main parameters used to characterise the extent of the π-back bonding to L — are concerned. Only in the case of the CO complex does the computed structure not agree perfectly with the experimental structure: the Pt−N(2) distance and the N(1)−Pt−L angle are greater in the calculated than in the experimental geometries (by 0.10 Å and 10°, respectively). However, it should be mentioned that a change in the N(1)−Pt−C angle of 10° causes only a small change in the total energy (a few kJ/mol). For the Pt−L distances greater differences between calculated and experimental values (Table 3) have been observed for the sulfur- and phosphorus-donor ligands, but this is mainly due to the neglecting of correlation effects in the calculations. The fact that the calculations reproduce the experimental geometries correctly indicates that the electronic structure of each complex has been described in a satisfactory way even at the HF level.

Table 3. Optimal geometrical parameters for $[PtI_2(R_2\text{-}phen)(L)]$ complexes (distances in Å, angles in degrees)

L[a]		Pt−N1	Pt−N2	N1−Pt−L	Pt−L
C_2H_4	exp.	2.24	2.24	143[b]	1.96
	calcd.	2.29	2.29	143[b]	2.14
C_2R_2[c]	exp.[d]	2.28	2.28	143[b]	2.01
	calcd.	2.29	2.29	143[b]	2.16
CO	exp.[e]	2.16	2.48	163	1.81
	calcd.	2.11	2.59	172	1.93
PR_3 [c]	exp.[e]	2.18	2.66	166	2.19
	calcd.	2.12	2.65	172	2.36
$(CH_3)_2SO$	exp.	2.11	2.63	171	2.20
	calcd.	2.05	2.65	178	2.47
$(CH_3)_2S$	exp.	2.09	2.67	170	2.26
	calcd.	2.07	2.64	173	2.47
C_5H_5N	exp.	2.04	2.68	177	2.03
	calcd.	2.08	2.67	171	2.12
H_2NR[f]	exp.	2.04	2.64	179	2.03
	calcd.	2.08	2.67	176	2.06

[a] R = H in the theoretical investigation (phen) and Me in the X-ray structural investigations (Me_2phen). [b] With respect to the midpoint of the C−C bond. [c] R = H in the theoretical and C_6H_5 (phenyl) in the X-ray structural investigation. [d] Experimental values.[8] [e] Experimental values.[5] [f] R = H in the theoretical and C_3H_7 (*n*-propyl) in the X-ray investigation.

An energy decomposition technique, the CSOV method,[16,17] has been employed to analyze the HF wave function and to identify the relative values of the charge transfer from L to the PtI_2(phenanthroline) residue (hereafter referred to as σ-donation) and of the reverse process, charge transfer from PtI_2(phenanthroline) to L (π back-donation). The interaction energy of the complex is divided into the sum of intra-unit polarization and charge-transfer contributions. Details of the procedure are not given here and can be found elsewhere.[16,18] The extent of charge transfer can be deduced from two independent parameters: the first one is the contribution of each charge-transfer process to the interaction energy (E_{int} in $kJ{\cdot}mol^{-1}$), and the second parameter is related to a wavefunction property, the dipole moment. With the assumed orientation of the I−Pt−I atoms along the x axis and the N−Pt−L groups along the y axis, the change in the y component of the dipole moment μ at each CSOV step ($\Delta\mu$) provides a direct measure of the charge flow from L to Pt and vice versa: a positive $\Delta\mu$ value indicates donation, a negative $\Delta\mu$ indicates back-donation. This is a much more reliable measure of the charge transfer than, for instance, the Mulliken charge.[18] Still, one has to keep in mind the qualitative nature of this partitioning.

The CSOV analysis allows the evaluation of the donating/back-donating properties of the ligands considered here (Table 4). As far as the donor properties are concerned, all ligands are good electron donors, as would be expected given the +2 formal oxidation state of the Pt atom. In more detail, the E_{int} values can be grouped into two domains: 180−230 and 130−160 $kJ{\cdot}mol^{-1}$. Similarly, two ranges of $\Delta\mu$ values are clearly distinguishable: 0.59−0.65 (with a peak of 0.91 for PH_3) and 0.46−0.47 au. Therefore PH_3, CO, C_2H_2, and C_2H_4 are the strongest donors both from the E_{int} and $\Delta\mu$ values. In contrast C_5H_5N and NH_3 are the poorest donors in the series both from E_{int} and $\Delta\mu$. $(CH_3)_2SO$ and $(CH_3)_2S$ lie between the two groups since they fall in the group of poor donors according to E_{int} but in the group of strong donors according to $\Delta\mu$.

Table 4. Donation and back-donation contributions in [PtI_2(phen)(L)] complexes as derived from a CSOV analysis; E_{int} is the contribution to the total interaction energy and $\Delta\mu$ the change in dipole moment associated with the donation or back-donation mechanisms

	Donation		Back-donation	
L	E_{int} (kJ/mol)	$\Delta\mu$ (au)	E_{int} (kJ/mol)	$\Delta\mu$ (au)
C_2H_4	219	+0.61	175	−0.93
C_2H_2	181	+0.59	154	−0.80
CO	230	+0.61	93	−0.46
PH_3	207	+0.91	48	−0.23
$(CH_3)_2SO$	143	+0.65	39	−0.23
$(CH_3)_2S$	132	+0.63	32	−0.13
C_5H_5N	160	+0.46	51	−0.43
NH_3	146	+0.47	23	−0.11

The π-acceptor properties, on the other hand, are quite different for the various ligands; moreover in this case both E_{int} and $\Delta\mu$ give very similar descriptions (E_{int} was chosen in drawing Figure 8). Acetylene and ethylene exhibit the strongest back-donating contributions. CO is halfway in between the alkene and the alkyne on one side and the amine ligand on the other. All other ligands fall in between the CO and the amine. The direct correlation between the π-acidity of the L ligand, as determined by the CSOV analysis, and the coordination mode of the phenanthroline ligand is surprising: bidentate when L is a good π-acceptor able to decrease the electron density in the trigonal plane, monodentate in most of the other cases with the CO positioned halfway in between the two extremes (Figure 8).

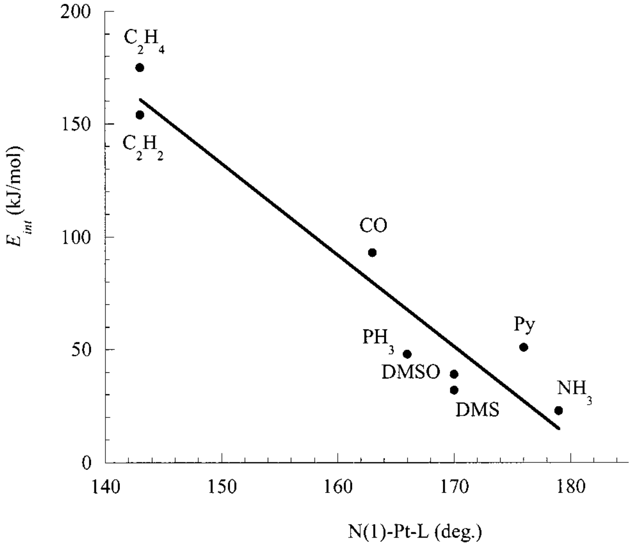

Figure 8. Plot of the computed π-acceptor ability of the L ligands (interaction energy E_{int}, Table 4) versus the experimental values of the N(1)−Pt−L angle (Table 3)

3. Discussion and Conclusion

The [PtI_2(Me_2-phen-N,N')] system is characterized by an extremly high steric interaction between the *ortho* substituents of the phenanthroline and the *cis* halogen ligands.[3−7] The steric constrictions within the square-planar geometry can be released by displacement of one end of the phenanthroline and addition of an extra ligand, forming a *trans*-[PtI_2(Me_2-phen-N)(L)] species. The coordinated Me_2-phen can then assume an orthogonal orientation with respect to the coordination plane so as to minimize the steric interactions with the *cis* ligands.

The coordination of the free end of the phenanthroline from the top side (the z direction assuming the square plane to be xy) is prevented by filled d orbitals of the metal lying in the same plane as the phenanthroline (d_{yz} and d_{z^2} electrons assuming as x direction that of the I−Pt−I vector).[19] However if the L ligand is a π-acid able to remove electron charge from the yz plane, the second end of the phenanthroline can also interact with the metal center and the complex switch from a square-planar four-coordinate to a trigonal-bipyramidal five-coordinate geometry comprising all possible intermediate situations. The X-ray technique is ideally suited for the observation of ground-state structures, particularly when intermolecular interactions are weak. This is the case here since the two large iodo ligands in *trans* positions (x axis) shield the yz plane, leaving the Me_2-phen ligand free to ride on the metal center and to assume the position which corresponds to the minimum of energy.

Therefore a direct correlation appears to exist between the N(1)−Pt−L angle (180° in four-coordinate and 143° in five-coordinate environments) and the ability of the ligand to remove electron charge from the yz plane. Alkenes and alkynes are found to be among the best π-acids and lead to a regular five-coordinate species. On the other hand the CO ligand is found to have a π-acidity much weaker than that of alkenes and alkynes. In our opinion the main difference between CO and alkenes or alkynes is that in CO the π*-orbitals of the ligand are disposed end-on with respect to the metal center, while in the case of alkenes and alkynes the π*-orbitals are disposed side-on with respect to the metal. Therefore the overlap of the platinum d-orbitals with the π*-orbitals of the carbonyl ligand is smaller than that with the π*-orbitals of alkenes and alkynes.

As expected, the phosphane ligand is found to be a better π-acid than ligands with sulfur and nitrogen donor atoms.

There is no significant difference between sulfoxide and sulfide from a crystallographic point of view, although theoretical calculations indicate a slightly better π-electron acceptor capacity for the sulfoxide.

The difference between pyridine and *n*-propylamine is also rather small [N−Pt−L angles of 176.5(2)° and 178.6(3)° for C_5H_5N and $H_2(C_3H_7)N$, respectively]. This small difference contrasts with the theoretical calculations reporting a π-acidity for pyridine similar to that of the phosphane. A very likely explanation for this apparent contradiction is that the N−Pt−L angle measures the ability of the L ligand to remove electron charge only from the yz plane and, for steric constrictions, such an ability is very small for pyridine. In fact, in order to reduce the steric interaction with the *cis* ligands, the plane of the pyridine will tend to be orthogonal to the coordination plane (xy plane) and, as a consequence, the empty π*-orbitals of the pyridine will be set roughly orthogonal to the yz plane and therefore will be unable to remove electron density from the platinum d-orbitals lying in this plane. In contrast, theoretical calculations measure the overall back-donation from platinum to L and this can be significant for pyridine due to the circumstances that the empty π*-orbitals of the pyridine are coplanar with the filled d_{xy} orbital of the metal. Therefore, for a pyridine oriented *quasi* orthogonal to the coordination plane, only the X-ray structural analysis gives an accurate description of the electron-acceptor ability of this ligand with respect to metal d-electrons localized in the yz plane. The same molecular device also allows a direct measure of the free-energy difference between ground state (four-coordinate species with singly bonded Me_2-phen) and transition state (five-coordinate species with doubly bonded Me_2-phen) when the former configuration is sufficiently low in energy to allow detection, by NMR spectroscopy, of different signals for the two inequivalent halves of the Me_2-phen ligand. By measuring the rate constants at different temperatures for the exchange between the two ends of singly bonded Me_2-phen, it is possible to evaluate $\Delta G^{\ddagger}_{T}$ ($\Delta G^{\ddagger}_{T} = \Delta G^{\ddagger}$ at the temperature T). In the case of the two amine ligands considered here the calculated values of $\Delta G^{\ddagger}_{295}$ (51 ± 2 and 52 ± 2 kJ·mol^{-1} for pyridine and *n*-propylamine, respectively) are very similar and in good agreement with the similar π-acceptor capacities deduced from X-ray data.

It cannot be excluded, however, that the possibility that, by using bidentate ligands with a lower tendency to act as a chelate than 2,9-dimethyl-1,10-phenanthroline, it is possible to destabilize the five-coordinate geometry to such an extent that the rate of exchange between free and coordinated ends of the bidentate ligand becomes observable by NMR spectroscopy also for compounds having L ligands with higher π-acidity than amines.

4. Experimental Section

Starting Materials: Commercial reagent-grade chemicals, 2,9-dimethyl-1,10-phenanthroline (Me_2-phen), ethylene (C_2H_4) (**a**), dimethyl sulfoxide (DMSO) (**e**), dimethyl sulfide (DMS) (**f**), pyridine (py) (**g**), and *n*-propylamine (NH_2Pr^n) (**h**), were purchased from Aldrich and used without further purification. [$PtI_2(Me_2$-phen)] (**1**) was prepared by a previously reported procedure.[3]

Preparation of *trans*-[$PtI_2(Me_2$-phen)(L)] Complexes (2): For L = C_2H_4 (**2a**) a rubber bladder filled with ethylene gas was connected to a flask containing a solution of [$PtI_2(Me_2$-phen)] (**1**) (0.3 mmol) in CH_2Cl_2 (20 mL).[5] After 30 minutes stirring, addition of diethyl ether to the mixture caused the precipitation of a red solid which was collected, washed with diethyl ether, and dried in air, yield 90%. $C_{16}H_{16}I_2N_2Pt$ (**2a**; 685.2): calcd. C 28.1, H 2.4, N 4.1; found C 28.4, H 2.1, N 4.0.

The complexes with L = DMSO (**2e**) and DMS (**2f**) were synthesized according to a procedure reported previously.[8] Yield 90%. $C_{16}H_{18}I_2N_2OPtS$ (**2e**; 735.3): calcd. C 26.1, H 2.5, N 3.8; found C 26.2, H 2.6, N 3.7. $C_{16}H_{18}I_2N_2PtS$ (**2f**; 719.3): calcd. C 26.7, H 2.5, N 3.9; found C 26.7, H 2.6, N 3.8.

The complexes with L = py (**2g**) and NH_2nPr (**2h**) were synthesized by addition of a dichloromethane solution of the L ligand (0.3 mmol in 5 mL of solvent) to a solution containing the stoichiometric amount of [$PtI_2(Me_2$-phen)] (0.3 mmol) in the same solvent (15 mL). After 2 minutes stirring, addition of diethyl ether to the mixture caused the precipitation of a dark-red solid which was collected, washed with diethyl ether, and dried in air, yield 90%. $C_{19}H_{17}I_2N_3Pt$ (**2g**; 736.2): calcd. C 31.0, H 2.3, N 5.7; found C 30.8, H 2.4, N 5.5. $C_{17}H_{21}I_2N_3Pt$ (**2h**; 716.3): calcd. C 28.5, H 3.0, N 5.9; found C 28.3, H 3.1, N 5.7.

Crystals of the compounds suitable for X-ray structure determinations were obtained from solutions of the platinum complexes in chloroform. Diethyl ether was gently stratified upon the above solutions in order to induce crystallization.

Physical Measurements: ^1H NMR spectra were recorded on a Bruker AM 300 instrument equipped with a temperature control unit; the data are reported in Table 1. The spectral simulation was performed using D NMR6.[20] The methyl protons of the 2,9-substituted phenanthroline were used to analyse the exchange between the free and coordinated ends of singly bonded Me$_2$-phen (flipping of the Me$_2$-phen ligand) in compounds **2g** and **2h**. Values of $\Delta H^{\ddagger}$ and $\Delta S^{\ddagger}$ were calculated from plots of ln(k/T) against $1/T$. IR spectra were recorded as KBr pellets on Perkin−Elmer 283 and FT 1600 spectrophotometers.

X-ray Data Collection, Structure Determination, and Refinement for Complexes 2a, 2e, 2f, 2g, and 2h: The crystallographic data are summarized in Table 5. Accurate unit-cell parameters were determined by least-squares refinement of the setting angles of 30 randomly distributed and carefully centerd reflections with θ in the range 10−20°. The data collections were performed at 293 K on a Siemens AED diffractometer by using the $\theta/2\theta$ scan mode. One standard reflection was monitored every 100 measurements, no significant decay was noticed over the time of data collection for all the compounds. The structures were solved by direct methods (SIR92)[21] and refined by full-matrix least-squares based on F_o^2 (**2a**, **2f**, and **2h**) or F_o (**2e** and **2h**) using the SHELXL-97 program,[22] first with isotropic then with anisotropic thermal parameters for all the non-hydrogen atoms. A semi-empirical method of absorption correction was applied for all the compounds (maximum and minimum values for the transmission coefficient were 1.000 and 0.904 for **2a**, 1.000 and 0.903 for **2e**, 1.000 and 0.725 for **2f**, 1.000 and 0.908 for **2g** and 1.000 and 0.937 for **2h**).[23,24] All the hydrogen atoms were placed at their geometrically calculated positions and refined as "riding" on their parent carbon or nitrogen atoms, except those of the ethylene (**2a**), which were found and refined isotropically. For compound **2h** the methyl group of the propylamine ligand was found to be disordered over two positions with occupancy factors of 0.66 and 0.34, respectively.

CCDC-216146 to -216150 (**2a**, **2e**, **2f**, **2g**, and **2h**, respectively) contain the supplementary crystallographic data for this paper. These data can be obtained free of charge via www.ccdc.cam.ac.uk/conts/retrieving.html (or from the Cambridge Crystallographic Data Centre, 12 Union Road, Cambridge CB2 1EZ, UK; Fax: (internat.) + 44-1223/336-033; or E-mail: deposit@ccdc.cam.ac.uk).

Computational Details: Ab initio calculations were performed to obtain an internally consistent measure of the π-acceptor ability of the L ligands. This was done according to an energy decomposition technique, the Constrained Space Orbital Variation (CSOV), implemented in the computer code HONDO 8.5[25] at the Hartree−Fock (HF) level. For this reason the electronic structures of the *trans*-[PtI$_2$(phen)(L)] complexes were determined at the ab initio HF level. Recently, the CSOV method has been implemented also at the Density Functional Theory (DFT) level, and test calculations have shown that the qualitative trends obtained as to the extent of donation/back-donation processes are very similar at the HF and DFT levels.[26] Therefore we expect the conclusions of this analysis not to be affected by the use of an HF wavefunction and to be valid in general. Except for the heavy atoms Pt and I, where an Effective Core Potential (ECP) was used, all other atoms were treated at the all-electron level. 68- and 46-Electron relativistic ECP's were used for Pt and I, respectively.[27] The 2,9-dimethyl-1,10-phenanthroline ligand (Me$_2$-phen) was represented by a 1,10-phenanthroline (phen). The L ligands considered were: C$_2$H$_4$, C$_2$H$_2$, CO, H$_3$P, (CH$_3$)$_2$SO, (CH$_3$)$_2$S, C$_5$H$_5$N, and H$_3$N. The ligands actually present in the real compounds were: C$_2$H$_4$, C$_2$(C$_6$H$_5$)$_2$, CO, (C$_6$H$_5$)$_3$P, (CH$_3$)$_2$SO, (CH$_3$)$_2$S, C$_5$H$_5$N, and H$_2$(C$_3$H$_7$)N. Therefore in the calculation procedure alkyl and phenyl substituents were represented by H atoms to reduce the computational burden. In the analysis of the results one has to take into account that some small differences between theory and experiment can be due to the use of simplified ligands in the calculations. The basis sets were of double-zeta quality for the ECPs of the Pt and I atoms,[27] for the C and N atoms directly bound to Pt, and for the P and S atoms.[28] Polarization functions (d),[29] particularly important for second-row

Table 5. Summary of the X-ray Crystallographic Data for **2a**, **2e**, **2f**, **2g**, and **2h**

Compound	[PtI$_2$(Me$_2$-phen)-(C$_2$H$_4$)] **(2a)**	[PtI$_2$(Me$_2$-phen)-(DMSO)] **(2e)**	[PtI$_2$(Me$_2$-phen)-(DMS)] **(2f)**	[PtI$_2$(Me$_2$-phen)-(py)] **(2g)**	[PtI$_2$(Me$_2$-phen)-(NH$_2$Pr^n)] **(2h)**
Empirical formula	C$_{16}$H$_{16}$I$_2$N$_2$Pt	C$_{16}$H$_{18}$I$_2$N$_2$OPtS	C$_{16}$H$_{18}$I$_2$N$_2$PtS	C$_{19}$H$_{17}$I$_2$N$_3$Pt	C$_{17}$H$_{21}$I$_2$N$_3$Pt
Molecular weight	685.20	735.27	719.27	736.25	716.26
Crystal system	triclinic	triclinic	triclinic	triclinic	monoclinic
Space group	$P\bar{1}$	$P\bar{1}$	$P\bar{1}$	$P\bar{1}$	$P2_1/c$
a (Å)	7.878(5)	13.908(8)	8.411(6)	9.715(5)	9.883(5)
b (Å)	9.231(5)	8.987(6)	9.143(7)	10.299(5)	13.168(7)
c (Å)	12.739(7)	8.211(6)	13.241(8)	11.682(6)	16.290(9)
α (°)	80.40(2)	75.69(2)	82.81(2)	79.87(2)	90
β (°)	75.09(2)	74.10(2)	78.46(2)	69.03(2)	106.53(2)
γ (°)	75.46(2)	82.86(2)	76.85(2)	67.40(2)	90
V (Å^3)	861.4(9)	954.6(11)	968.1(12)	1006.6(9)	2032.4(19)
Z	2	2	2	2	4
λ (Mo-$K\alpha$)	0.71073	0.71073	0.71073	0.71073	0.71073
ρ(calcd) (Mg/m^3)	2.642	2.558	2.467	2.429	2.341
μ (mm^{-1})	11.724	10.697	10.541	10.043	9.945
θ range (°)	3.17−30.04	3.05−30.06	3.04−30.00	3.48−27.04	3.03−27.07
No. of reflns/obsd $F > 4\sigma(F)$	5006/2886	5586/4235	5632/4112	4401/3739	4803/2588
GOOF [a]	0.944	1.009	1.197	1.049	0.929
$R1$[a]	0.0444	0.0414	0.0312	0.0316	0.0339
$wR2$[a]	0.1233	0.1047	0.0696	0.0880	0.0677

[a] GOOF = $\{\Sigma[w(F_o^2 - F_c^2)^2]/(n - p)\}^{1/2}$; $R1 = \Sigma||F_o| - |F_c||/\Sigma|F_o|$; $wR2 = \{\Sigma[w(F_o^2 - F_c^2)^2]/\Sigma[w(F_o^2)^2]\}^{1/2}$; $w = 1/[\sigma^2(F_o^2) + (aP)^2 + bP]$, $P = [\max(F_o^2,0) + 2F_c^2]/3$.

atoms like S and P,[18] were added to these atoms. All the remaining C and H atoms were treated by a MINI basis set.[30]

The geometry of the complexes was fully optimized by means of analytical gradients. Only one plane of symmetry was imposed: this is the plane containing the phenanthroline ligand and perpendicular to the straight line connecting the two iodo ligands (C_s symmetry). The L ligand was completely free to rotate and change position with respect to the phenanthroline. This is essential in order to guarantee that the calculations reproduce the correct geometry.

Acknowledgments

We thank the University of Bari, the Ministero dell'Istruzione Università e Ricerca (MIUR) (Cofin. N. 2001053898 and 2000 N. MMO3027791), the EC (COST Chemistry projects D20/0001/2000 and D20/0003/01) for support.

---

[1] F. Basolo, *Coord. Chem. Rev.* **1996**, *154*, 151−161, and references cited therein.

[2] F. A. Cotton, G. Wilkinson, C. A. Murillo, M. Bochmann. *Advanced Inorganic Chemistry*, 6th ed; Wiley-Interscience, John Wiley & Sons, New York, **1999**.

[3] F. P. Fanizzi, F. P. Intini, L. Maresca, G. Natile, M. Lanfranchi, A. Tiripicchio, *J. Chem. Soc., Dalton Trans.* **1991**, 1007−1015.

[4] R. J. H. Clark, F. P. Fanizzi, G. Natile, C. Pacifico, G. C. van Rooyen, D. A. Tocher, *Inorg. Chim. Acta* **1995**, *235*, 205−213.

[5] F. P. Fanizzi, L. Maresca, G. Natile, M. Lanfranchi, A. Tiripicchio, G. Pacchioni, *Chem. Commun.* **1992**, 333−335.

[6] F. P. Fanizzi, G. Natile, M. Lanfranchi, A. Tiripicchio, *Inorg. Chem.* **1994**, *33*, 3331−3339.

[7] F. P. Fanizzi, G. Natile, M. Lanfranchi, A. Tiripicchio, F. Laschi, P. Zanello, *Inorg. Chem.* **1996**, *35*, 3173−3182.

[8] F. P. Fanizzi, G. Natile, M. Lanfranchi, A. Tiripicchio, G. Pacchioni, *Inorg. Chim. Acta* **1998**, *275−276*, 500−509.

[9] A. Albinati, R. W. Kunz, C. J. Ammann, P. S. Pregosin, *Organometallics* **1991**, *10*, 1800.

[10] A. Gogoll, J. Ornebro, H. Grennberg, J. E. Bakwall, *J. Am. Chem. Soc.* **1994**, *116*, 3631−3632.

[11] R. Romeo, G. Alibrandi, *Inorg. Chem.* **1997**, *36*, 4822−4830.

[12] J. G. P. Delis, P. G. Aubel, K. Vrieze, P. W. N. M. van Leuwen, N. Veldman, A. L. Spek, F. J. R. van Neer, *Organometallics* **1997**, *16*, 2948.

[13] R. Romeo, L. Fenech, L. Monsù Scolaro, A. Albinati, A. Macchioni, C. Zuccaccia, *Inorg. Chem.* **2001**, *40*, 3293−3302.

[14] L. Lunazzi, G. Cerioni, K. U. Ingold, *J. Am. Chem. Soc.* **1976**, *98*, 7484−7488.

[15] K. G. Orrell, V. Sik, *Ann. Rep. NMR Spect.* **1993**, *27*, 103−171.

[16] P. S. Bagus, K. Hermann, C. W. Bauschlicher, *J. Chem. Phys.* **1984**, *80*, 4378−4386.

[17] P. S. Bagus, F. J. Illas, *Chem. Phys.* **1992**, *96*, 8962−8970.

[18] G. Pacchioni, P. S. Bagus, *Inorg. Chem.* **1992**, *31*, 4391−4398.

[19] Z. Lin, M. B. Hall, *Inorg. Chem.* **1991**, *30*, 646−651.

[20] D NMR6: *Calculation of NMR Spectra (I = 1/2) Subject to the Effects of Chemical Exchange.* J. H. Brown and C. H. Bushweller, University of Vermont, Burlington, Vermont, **1983**.

[21] A. Altomare, G. Cascarano, C. Giacovazzo, A. Gualiardi, M. C. Burla, G. Polidori, M. Camalli, *J. Appl. Crystallogr.* **1994**, *27*, 435−443.

[22] G. M. Sheldrick, SHELXL-97. *Program for Crystal Structure Determination.* University of Göttingen, Göttingen, Germany, **1997**.

[23] N. Walker, D. Stuart, *Acta Crystallogr., Sect. A* **1983**, *39*, 158−166.

[24] F. Ugozzoli, *Comput. Chem.* **1987**, *11*, 109−120.

[25] M. Dupuis, F. Johnston, A. Marquez, HONDO 8.5 for CHEMStation (IBM Co., Kingston, **1994**).

[26] A. M. Márquez, N. Lopez, M. García-Hernández, F. Illas, *Surf. Sci.* **1999**, *442*, 463−476.

[27] P. J. Hay, W. R. Wadt, *J. Chem. Phys.* **1985**, *82*, 270−283.

[28] J. Hehre, R. Ditchfield, J. A. Pople, *J. Chem. Phys.* **1972**, *56*, 2257−2261.

[29] *Gaussian Basis Sets for Molecular Calculations* (Ed.: S. Huzinaga), Physical Science Data, Vol. 16 (Elsevier, Amsterdam **1984**).

[30] H. Tatewaki, S. Huzinaga, *J. Comp. Chem.* **1980**, *1*, 205−228.

Received December 2, 2003